Military Technical College
Kobry El-Kobbah,
Cairo, Egypt.

17th International Conference on Applied Mechanics and Mechanical Engineering.

EXPERIMENTAL, COMPUTATIONAL, AND EMPIRICAL EVALUATION OF SUPERSONIC MISSILE AERODYNAMIC COEFFICIENTS

L. A. El-Mahdy[*], M. Y. M. Ahmed[*, 1], O. K. Mahmoud[*] and O. E. Abdel-Hameed[*]

ABSTRACT

One crucial step in design and development procedures of missiles is the estimation of their aerodynamic features. Practically, high fidelity techniques namely, experimental and computational and low-fidelity engineering techniques are all implemented within the framework of missile aerodynamic evaluation. The present work compares these three different techniques in the context of aerodynamic analysis of a conventional fin-stabilized tactical missile configuration. The flight conditions correspond to Mach numbers varying from 1.5 to 4 at incidence up to 18 degrees. The variation of lift and drag coefficients and center of pressure location with the flight conditions according to the three approaches are compared.

---

* Egyptian Armed Forces.

1 Email of Corresponding author: mym141101@yahoo.com

INTRODUCTION

It is of no doubt that none of the three aerodynamic evaluation approaches namely, engineering, numerical, and experimental can be totally put aside. That is because each has its own role in the design and development loop. Engineering empirical and semi-empirical techniques are adequate for conceptual and preliminary phases of design for their quick, yet least-accurate, outcome. More accurate results needed in further design phases can be obtained from computational and experimental aerodynamic evaluation approaches.

A huge body of researches discussing the aspects of missile aerodynamics can be found in the open literature [1-20], to name a few. In most of these studies, experimental, analytical, and computational approaches were compared in many applications. Empirical and experimental approaches were compared in [1-9] whereas in [10-17], computational results were compared with experimental measurements. Computational techniques were also compared with empirical ones in [18]. Comparative studies aggregating the three approaches were also conducted [19-20].

Maurice [19] compared the aerodynamic coefficients of an anti-aircraft missile of a conventional design whereas in Rosema el al. [20] implemented the three approaches in a comparative study on the aerodynamic coefficients of several missiles with strakes.

Experimental, computational, and empirical approaches in estimating the missile aerodynamic coefficients are compared in the present study in the context of exploring the aerodynamic characteristics of a conventional tactical missile at high Mach numbers and high angles of attack. The missile configuration is a cone-cylinder equipped with four trapezoidal stabilizing fins. The free stream Mach number varies from 1.5 to 4 at incidence angle varying from 4 to 18. The variation of the lift and drag coefficients and the center of pressure location of the missile are considered. The commercial CFD solver ANSYS [21] is utilized as the computational tool whereas the Missile DATCOM package [22] is implemented as the semi-empirical tool. For comparison, available experimental wind tunnel measurements conducted by the research group are used. In the following section, the case study and research methodology are discussed in detail. The main findings of the study are presented and discussed next followed by the key conclusions.

CASE STUDY AND METHODOLOGY

Case Study

The case study is a conventional cone-cylinder-fin-stabilized tactical missile with two outer conduits separated by 180^o and extend along the midsection. The model investigated experimentally is a 1: 16 scaled model of the missile with total length and caliber of 551.25 mm and 34 mm, respectively. Figure 1 shows the model investigated. The scope of the present study is the supersonic free stream conditions corresponding to Mach 1.5 to 4 and incidence angles 4^o to 18^o. The missile is assumed in flight with stabilizing fins at x-orientation such that the two conduits are on the windward and leeward sides of the missile.

Wind Tunnel Data

The aerodynamic characteristics of the model shown in Fig. 1 have been investigated experimentally by the research group [23]. The wind tunnel is a tri-sonic open tunnel, which test section dimensions are 0.6×0.6m^2 and the length is 1.575m. The available measurements correspond to test conditions ranging from Mach 0.4 to 4.45 and corresponding Reynolds number ranging from 8.7e6 to 26.5e6 (with model length taken as the reference length).

The attack angle mechanism can change the incidence angle in the range of –15°~38° and a sting balance mechanism (fitted internally to the model base) is utilized in measuring the aerodynamic loads on the model. Fig. 2 shows the model installation in the wind tunnel test section. Based on measurements, the model aerodynamic coefficients are calculated taking the reference length and area of 0.55125 m and 0.0009079 m^2, respectively. The accuracy of recorded data in measurements of the aerodynamic loads is maintained within ±1% of their nominal values [23].

Numerical Simulation Setup

To accurately replicate the wind tunnel experiments numerically, a computational domain identical to the test section of the wind tunnel is constructed. Since only the incidence angle is considered, the flow around the model is pitch-plane symmetric. Thus, only half 3D domains are constructed, as shown in Fig. 3. The sting used in wind tunnel experiments is added to the numerical model so as to replicate the flow conditions in the wind tunnel.

The upstream boundary of the domain is set to be pressure inlet where the gauge total pressure and the total temperature are defined as in the tunnel experimental data. The downstream boundary is defined as pressure outlet where the values of the gauge pressure and the total temperature are specified. The pitch plane is defined as symmetry plane with zero normal gradients of the flow properties whereas all model and sting surfaces are defined as non-slip walls. The wind tunnel walls are defined as slip walls on which no boundary layer is created numerically. Domain boundary definitions are shown in Fig. 3.

An unstructured tetrahedral grid is generated in the domain and its resolution is enhanced by applying two scoping methods; the body element sizing then the sphere of influence sizing. Body element sizing generates a clustered fine grid around the body surface only whereas the sphere of influence generates clustered areas inside the domain where key flow features such as shock and expansion waves are expected to take place. Here, five spheres of influence are drawn (marked by the thick circles in Fig. 4). The resulting grid is nearly feature-aligned as shown in Figure 4. A grid sensitivity check is applied and a grid with 1825562 cells is found to yield a grid-independent prediction of the aerodynamic coefficients.

The commercial CFD code ANSYS FLUENT [21] is utilized in the present study. It uses a cell-centered finite volume method and has been proven to work well for different flow regimes around missiles. The double-precision implicit density-based steady solver available in FLUENT is implemented in the present simulations along with a second-order special discretization scheme. Air is treated as ideal gas and Spalart-Allmaras turbulence model is implemented.

Semi-Empirical Prediction Code

Missile DATCOM [22] is an aerodynamic prediction computer code that developed by the USAF Flight Dynamics Laboratory since 1984. The code has proved to be capable of estimating the aerodynamic characteristics of missiles of conventional shapes with a high level of accuracy [8, 9, 18 - 20].

RESULTS AND DISCUSSIONS

Variation of the Total Lift Coefficient with the Free-stream Conditions

The dependence of model lift coefficient on the freestream conditions is illustrated in Figures (5 and 6). In Figures 5 (a, b and c), the variations of the experimental, numerical, and empirical results of lift coefficient with incidence are compared for sample values of Mach number.

For all Mach numbers, the measured lift coefficient increases with the increase in the angle of attack. The curves show coherence of the computational and analytical results to the experimental measured behavior with very small error values at low incidence and higher ones at high incidences. At extreme conditions namely, high Mach and incidence, CFD simulations results show better accuracy compared with those of the empirical tool. Fig. 6 aggregates the dependence of the model lift coefficient with the free-stream conditions, Mach and incidence values as estimated experimentally, numerically, and empirically. Clearly, lift coefficient is more sensitive to variation of incidence angle than that of the free-stream Mach value.

Variation of the Total Drag Coefficient with the Free-Stream Conditions

The dependence of the total drag coefficient of the model with the free-stream conditions is illustrated in Figures (7 and 8). In Figures 7 (a, b and c), the variations of the experimental, numerical, and empirical results of total drag coefficient with incidence are compared for sample values of Mach number.

Closely examining the Figures (7 and 8) show that drag decreases slightly with the increase in Mach value while it increases considerably with the incidence angle. Generally, the rise in drag with the incidence angle shows a steeper trend for $\alpha > 10^o$. As the incidence increases, the slope of this dependence increases monotonically. Compared with experimental values, the trend of results is better captured by CFD simulation results. CFD simulations give more accurate results than those given by empirical technique. This accuracy is more pronounced at higher Mach values than that at lower ones. The accuracy of DATCOM results is higher at incidence angles below 10^o and generally deteriorates at high Mach values. Fig. 8 aggregates the dependence of total drag coefficient, C_D, on the free-stream conditions namely, Mach number and incidence angle as estimated experimentally, computationally, and analytically. It is clear that the drag is more sensitive to the variation of incidence angle than to that of the free stream Mach number.

Variation of the Center of Pressure Position with the Free-Stream Conditions

The change in center of pressure location with the free-stream conditions is shown in Fig. 9. The centre of pressure distance measured from the model nose tip is normalized with respect to the model length.

At 1.5 Mach, experimental normalized centre of pressure shifts forward with the increase of the angle of attack. CFD and DATCOM results show the same trend with a small error. At Mach 3, a different behavior now appears from the CFD in a good agreement with the experimental measurements. The empirical tool does not show the same trend, the DATCOM results show continuously decreasing trend. Finally, at Mach 4, the normalized centre of pressure shifts downstream with the increase in the angle of attack. This is valid for the data obtained from experimental measurements, CFD results. DATCOM results show a contradicting trend, the centre of pressure shift forward with the increase of the angle of attack. Overall, with reference to measurements, CFD results seem to be more accurate than the empirical one in predicting both trend and values of the model pressure centre location. Fig. 10 aggregates the dependence of model pressure center location on the flight conditions namely, Mach number and incidence angle. The attitude of moving backward beyond Mach 3 for 10^o incidence, beyond Mach 2.5 for 14^o incidence and Mach 2 for 18^o incidence is exclusively captured by CFD simulations in agreement with wind tunnel measurements. Missile DATCOM fails to capture the same trend.

DATCOM results predict the expected trend of pressure centre location namely, shifting upstream as the cross flow velocity component ($M_\infty \, sin\alpha$) increases. So, by increasing either Mach number of angle of attack, DATCOM predicts that the center of pressure locations moves towards the missile nose. However, the experimental measurements as well as the numerical simulations predict another trend especially for high Mach or angles of attack. In these conditions, the centre of pressure was found (experimentally and computationally) to shift downstream rather than upstream at certain free stream conditions. An explanation to this trend is attempted here. As the cross-flow velocity increases, the flow separation on the missile tail section (including the fins) becomes more significant. This, in addition to the increased normal force due to viscous flow, may cause the rise of tail section contribution to the total normal force on the complete missile. This explanation may be supported by the results reported in Figure 5 where DATCOM predicts lower total lift coefficient compared with experimental and computational ones. Since Datcom does not simulate the flow and, rather, predicts the aerodynamic coefficients based on a set of theory-based formula, it may not be able to predict the real flow behavior at these extreme conditions. In fact, according to the user manual of DATCOM [22], the prediction accuracy of the code is limited to small angles of attack.

CONCLUSIONS

The focus of the present study was to estimate the aerodynamic characteristics of a conventional fin-stabilized missile configuration. The objective was to compare the capabilities of prediction and accuracy of missile aerodynamic coefficients using three approaches namely experimental, computational, and empirical. Free-stream conditions corresponding to high supersonic Mach numbers (up to 4) and high angles of attack (up to 18) were examined. It was concluded that CFD simulations have the capability of predicting the aerodynamic coefficients and features with relatively higher accuracy compared to that obtained by empirical tools. This is more pronounced at high supersonic Mach numbers. Missile DATCOM code presented results with good accuracy as compared to that of the experimental. It has been proved, in many ways, that the location of pressure centre of the missile investigated shows a special behavior. At low incidence, as the Mach number increases, the centre of pressure shifts towards the model nose. At higher incidence angles, as the Mach number increases, the pressure centre shifts upstream (towards the model nose) and then downstream. The value of the free-stream Mach number beyond which the pressure centre location starts to migrate downstream decreases as the incidence angle increases. This behavior of pressure centre location has been captured by experimental measurements, CFD simulations but it wasn’t captured by the DATCOM.

REFERENCES

[1] F. A. Woodward, "Analysis and design of wing-body combinations at subsonic and supersonic speeds," *Journal of aircraft,* vol. 5, pp. 528-534, (1968).

[2] W. C. Y. Oberkamp and J. C. Y. Nicolaides, "Aerodynamics of finned missiles at high angle of attack," *AIAA journal,* vol. 9, pp. 2378-2384, (1971).

[3] W. Blake, "Missile Datcom- Applications to projectiles," in *AIAA Atmospheric Flight Mechanics Conference, Boston, MA*, pp. 212-221, (1989).

[4] E. H. Smith, S. K. Hebbar, and M. F. Platzer, "Aerodynamic characteristics of a canard-controlled missile at high angles of attack," *Journal of spacecraft and rockets,* vol. 31, pp. 766-772, (1994).

[5] J. White, "An assessment of missile DATCOM prediction accuracy relative to generic Body+ Wing+ Tail missile pitch aerodynamics," *AIAA paper,* pp. 95-1893, (1995).
[6] F. Moore and T. Hymer, "Improved methodology for axial force prediction at angle of attack," *Journal of Spacecraft and rockets,* vol. 35, pp. 132-139,(1998).
[7] Habip and A. Mehmet, "Prediction of Aerodynamic Characteristics of Missiles with Circular and Noncircular Cross Sections," *Turkish Journal of Engineering and Environmental Sciences,* vol. 23, pp. 149-160, (1999).
[8] E. J. Abney and M. A. McDaniel, "High angle of attack aerodynamic predictions using missile datcom," *AIAA paper* 2005-5086, (2005).
[9] T. J. Sooy and R. Z. Schmidt, "Aerodynamic predictions, comparisons, and validations using missile Datcom (97) and aeroprediction 98 (AP98)," *Journal of spacecraft and rockets,* vol. 42, pp. 257-265, (2005).
[10] O. Baysal, K. Fouladi, and D. Miller, "Computations of supersonic flows over a body at high angles of attack," *AIAA journal,* vol. 27, pp. 427-437, (1989).
[11] T. Birch, D. Ludlow, N. Qin, and B. DERA, "Towards an efficient, robust and accurate solver for supersonic viscous flows," in *Proceedings of the ICAS 2000 Congress, Harrogate, UK*, (2000).
[12] J. Sahu, K. Heavey, and S. Dinavahi, "Application of CFD to high angle of attack missile flow fields," *Chimera,* vol. 10, p. 11, (2000).
[13] S. B. Khelil, P. Guillen, M. Lazareff, and R. G. Lacau, "Numerical simulation of roll induced moment of cruciform tactical missiles," *Aerospace Science and Technology,* vol. 5, pp. 109-124, (2001).
[14] S. Deck, P. Duveau, P. d'Espiney, and P. Guillen, "Development and application of Spalart–Allmaras one equation turbulence model to three-dimensional supersonic complex configurations," *Aerospace Science and Technology,* vol. 6, pp. 171-183, (2002).
[15] J. DeSpirito, M. Vaughn, and W. D. Washington, "CFD investigation of canard-controlled missile with planar and grid fins in supersonic flow," *AIAA paper,* vol. 4509, (2002).
[16] X. Liu and S. Fu, "Numerical simulation of compressible separated turbulent flows over inclined slender body," *Journal of spacecraft and rockets,* vol. 42, pp. 572-575, (2005).
[17] H. H. Al-Kayiem, A. K. Hussein, J. M. Jaleel, and S. H. Hussain, "Numerical Computation of 3-dimensional Supersonic Flow Field over Seamless Missiles," *Indian Journal of Science and Technology,* vol. 7, pp. 1563-1572, (2014).
[18] Ridluan, "CFD Investigation of Compressible Low Angles of Attack Flow over the Missile," *Journal of Physical Science and Application,* vol. 4, pp. 339-347, (2014).
[19] F. Maurice, "Aerodynamic performance predictions of a SA-2 Missile using Missile Datcom," Monterey, California. Naval Postgraduate School, (2009).
[20] C. Rosema, E. Abney, S. Westmoreland, and H. Moore, "A Comparison of Predictive Methodologies for Missile Configurations with Strakes," in *33rd AIAA Applied Aerodynamics Conference*, (2015).
[21] ANSYS Fluent 14.5.7, User Guide.
[22] Blake, W. B., “Missile DATCOM: User’s Manual 1997 Fortran 90 Revision,” U.S. Air Force Research Lab. Air Vehicles Directorate, Wright–Patterson AFB, OH, Feb. (1998).
[23] DSSC, "Technical ReportDSSC-TR70120,” (2012).

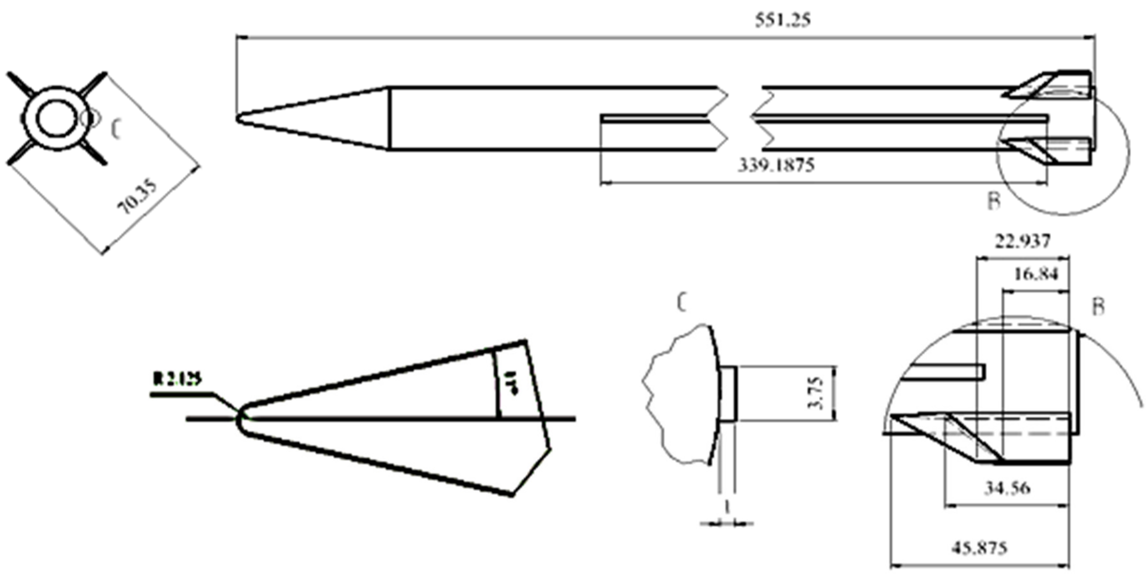

Figure 1. Model configuration.

Figure 2. Model installation in the wind tunnel test section.

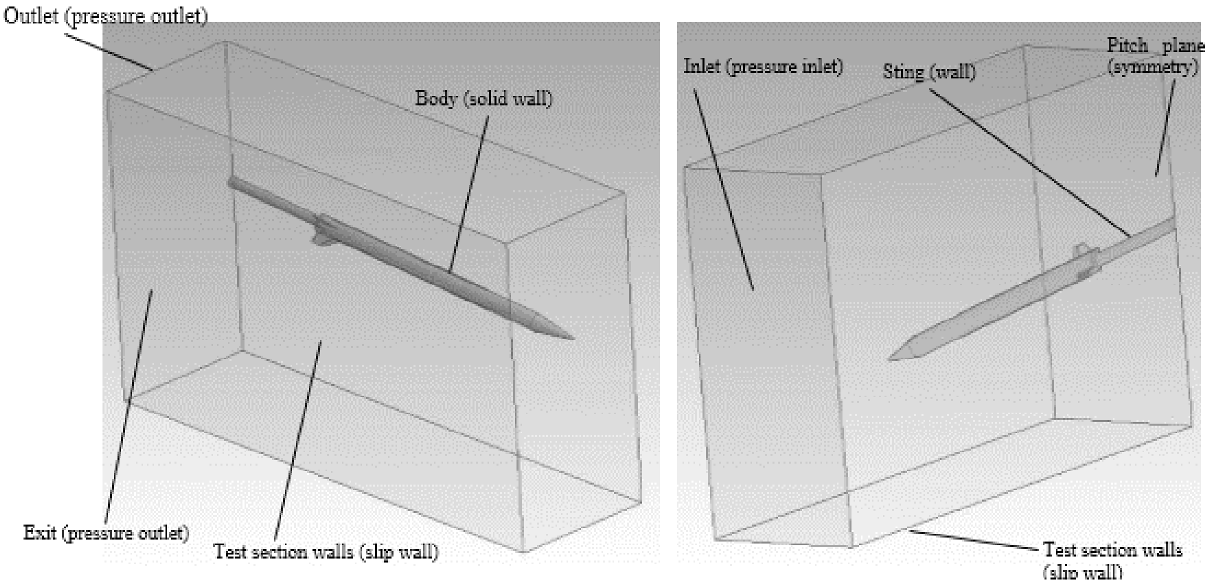

Figure 3. Bounded domain configuration and boundary definitions.

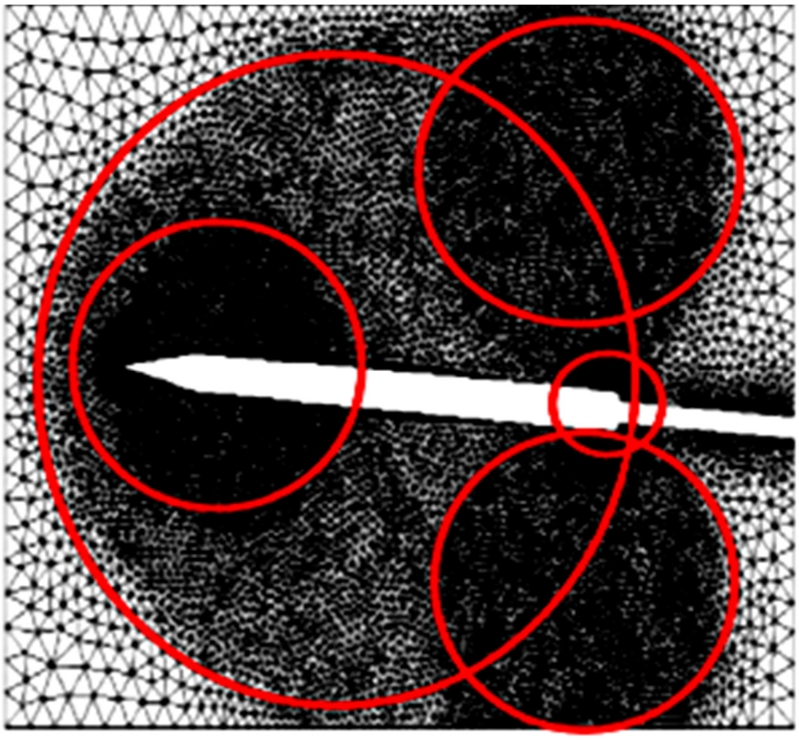

Figure 4. Domain discretization using sphere of influence scoping method.

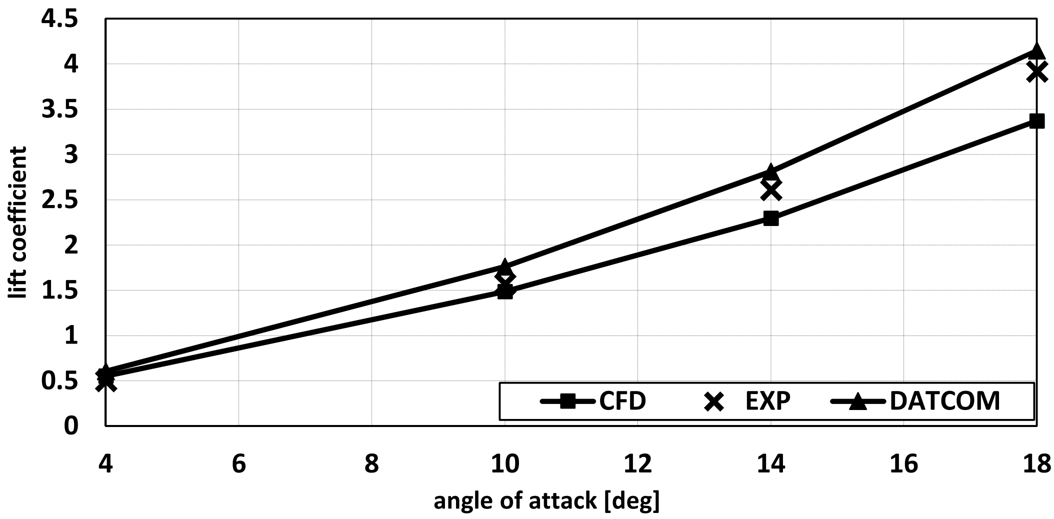

(a) 1.5 Mach

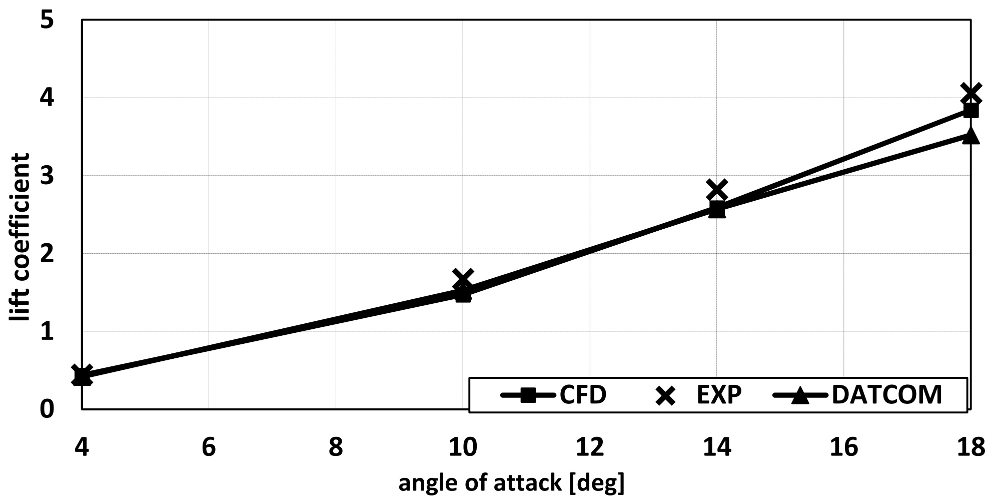

(b) 3 Mach

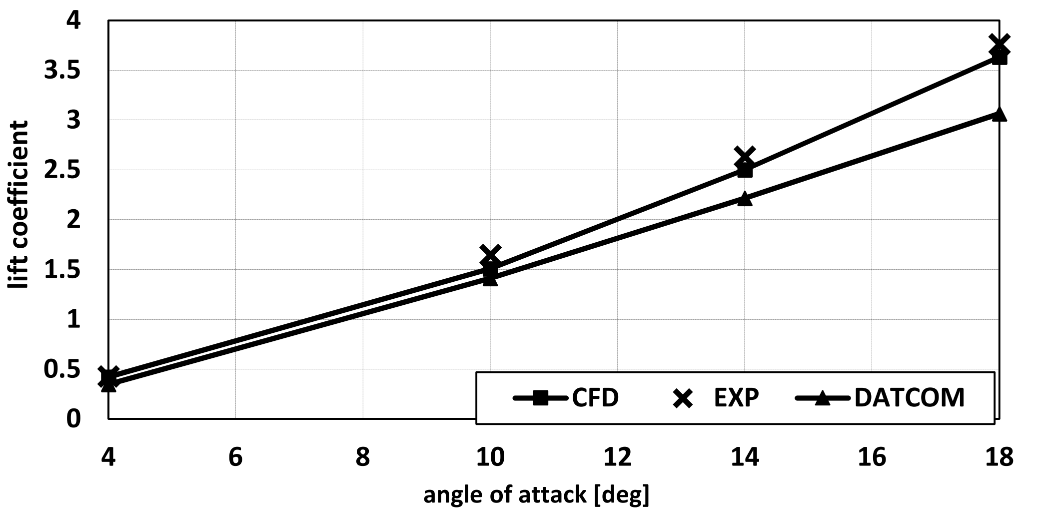

(c) 4 Mach

Figure 5. Variation of lift coefficient C_L with incidence at different free-stream Mach numbers.

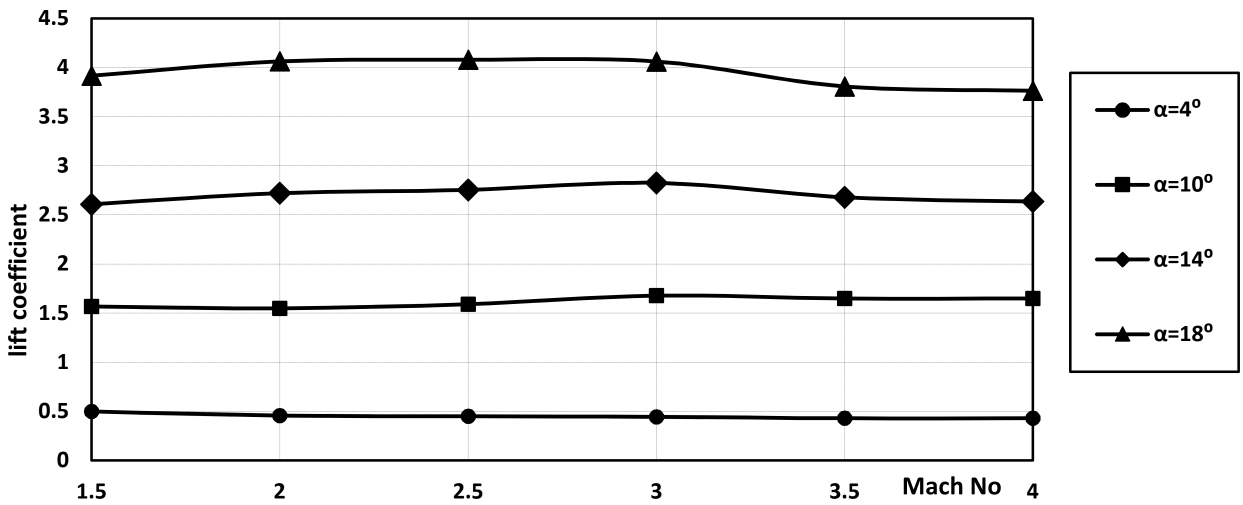

(a) Experimental

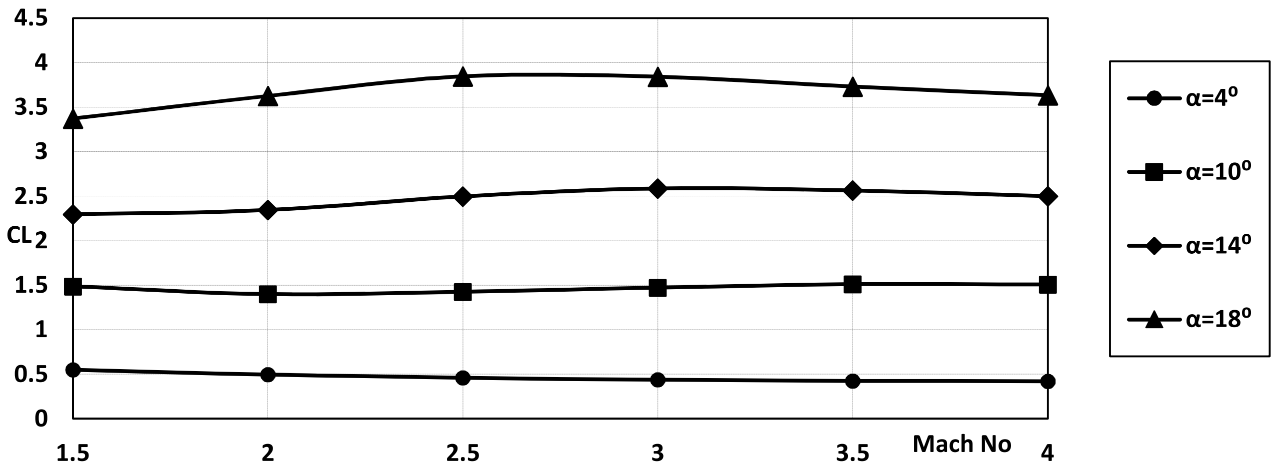

(b) Computational

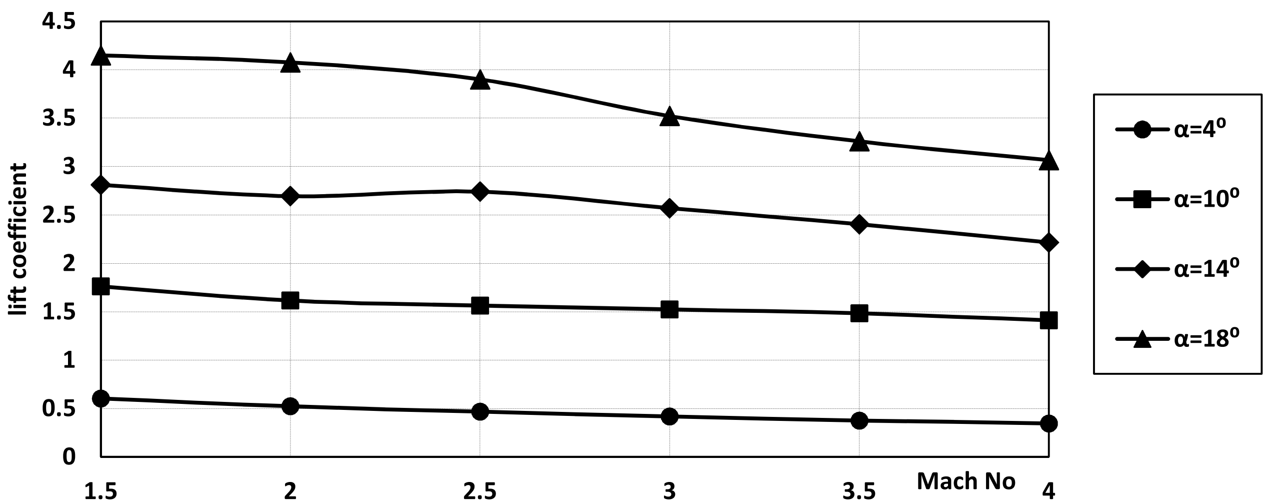

(c) DATCOM

Figure 6. Variation of lift coefficient C_L with the Mach number at different angles of attack.

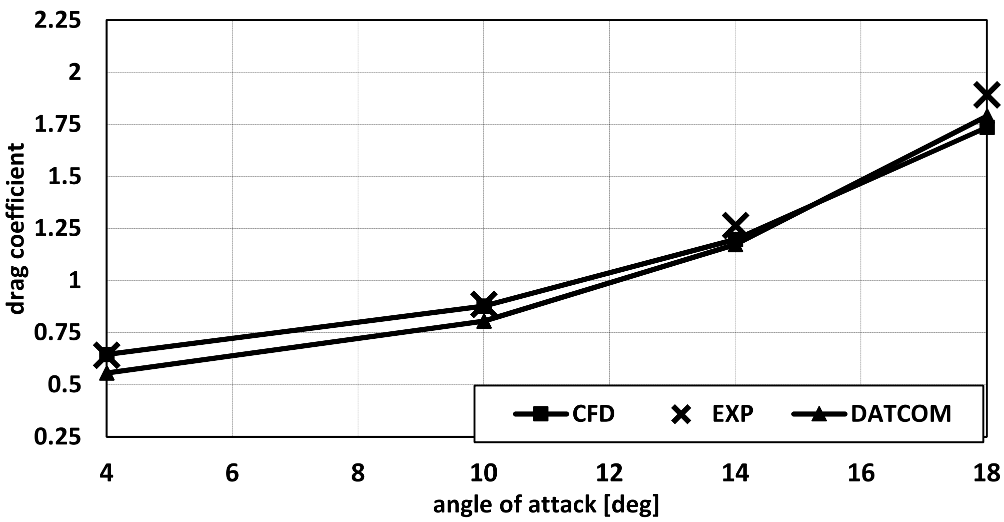

(a) 1.5 Mach

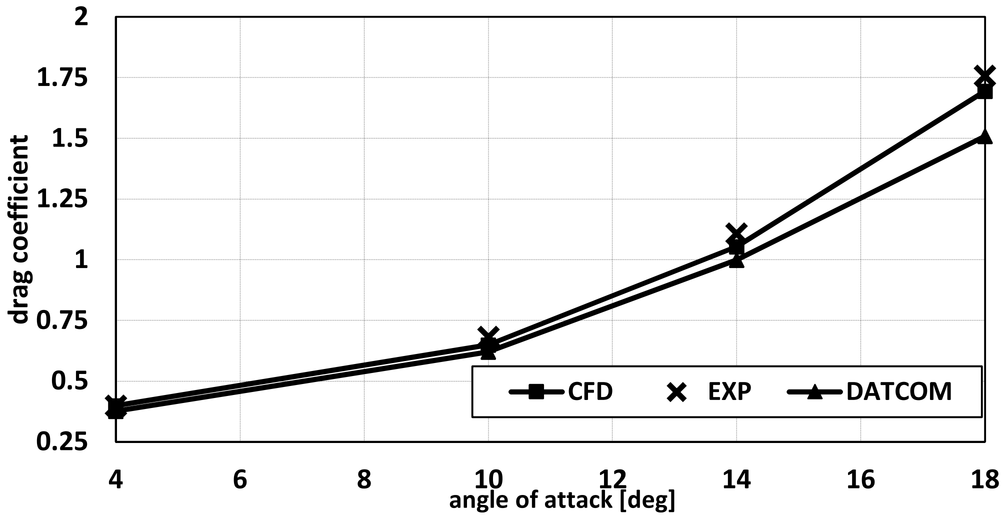

(b) 3 Mach

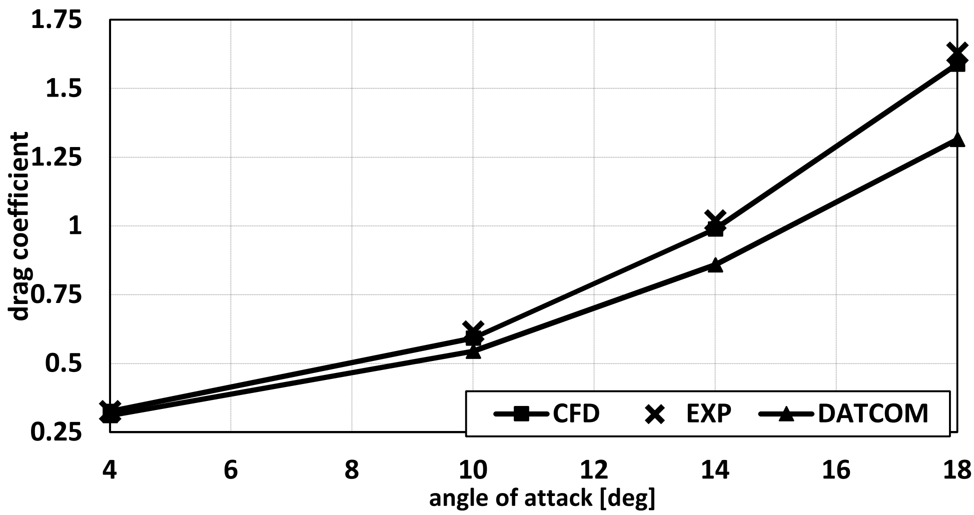

(c) 4 Mach

Figure 7. Variation of total drag coefficient C_D with incidence at different free-stream Mach values.

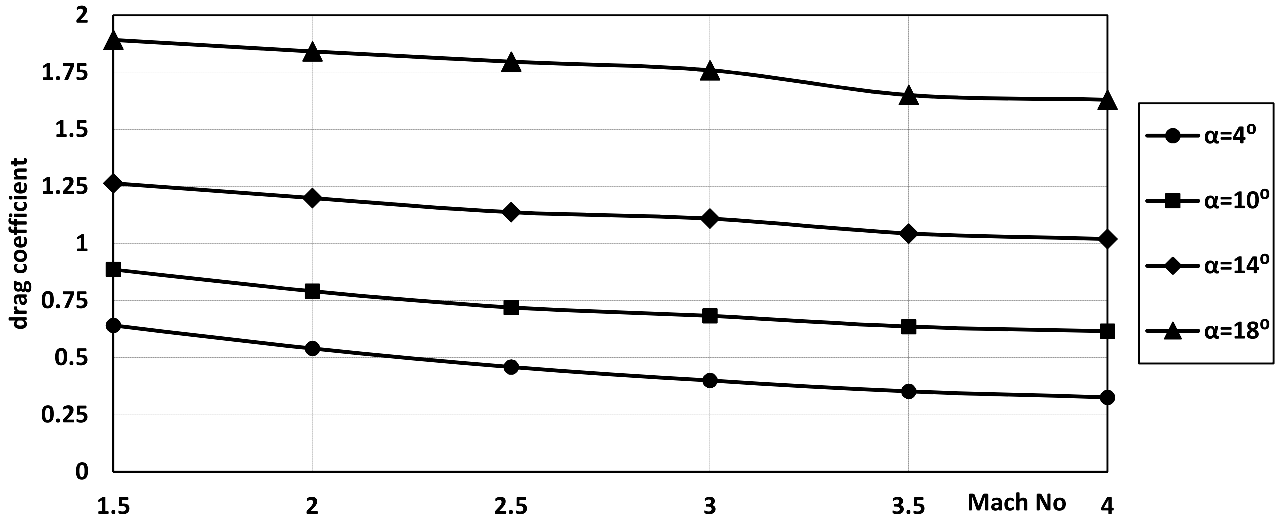

(a) Experimental

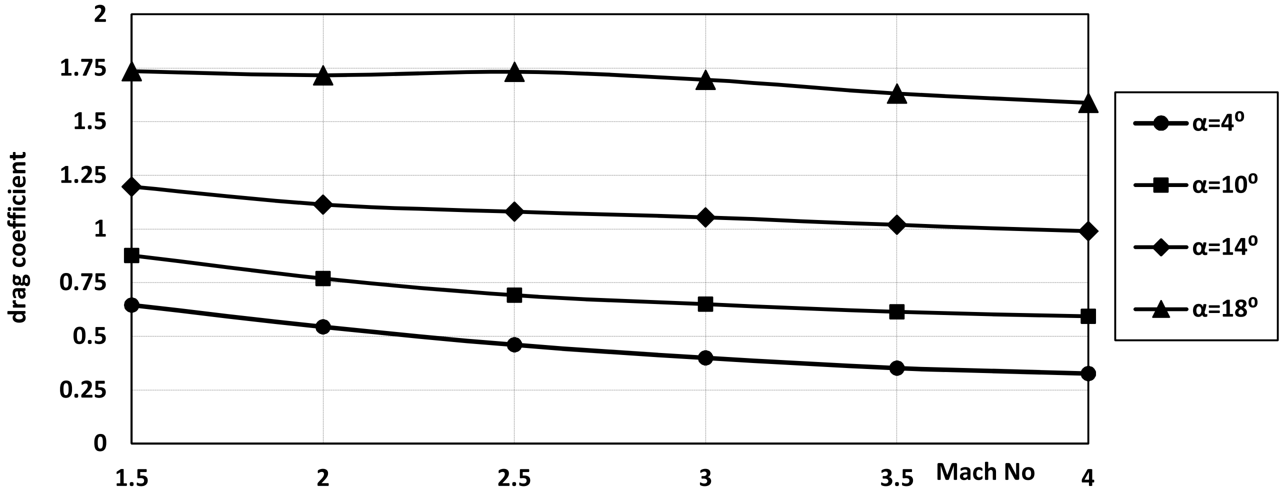

(b) Computational

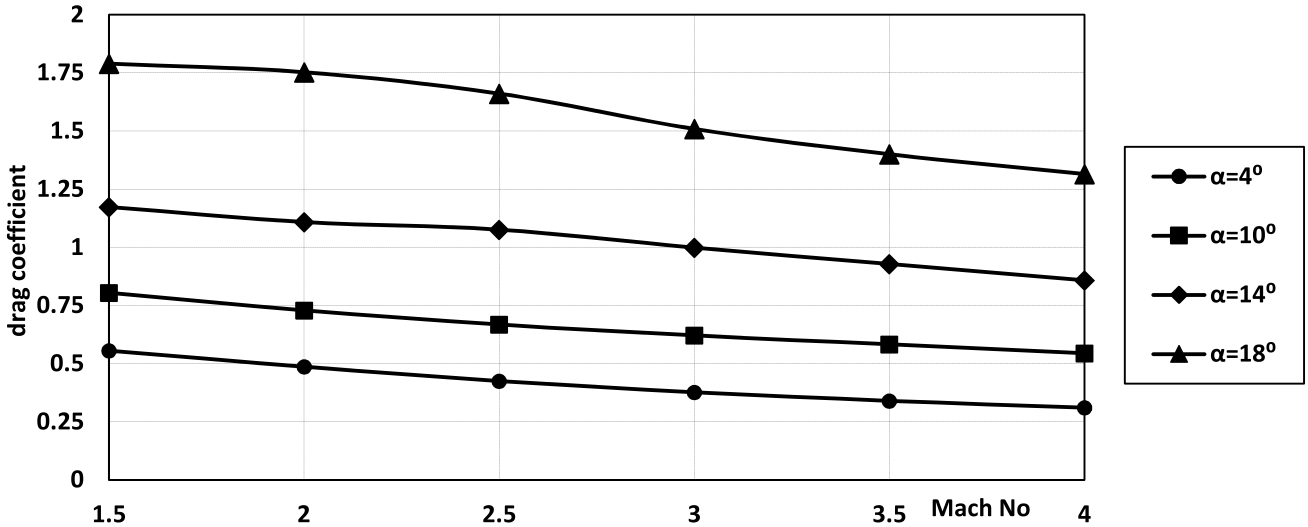

(c) DATCOM

Figure 8. Variation of drag coefficient C_D with the Mach number at different angles of attack.

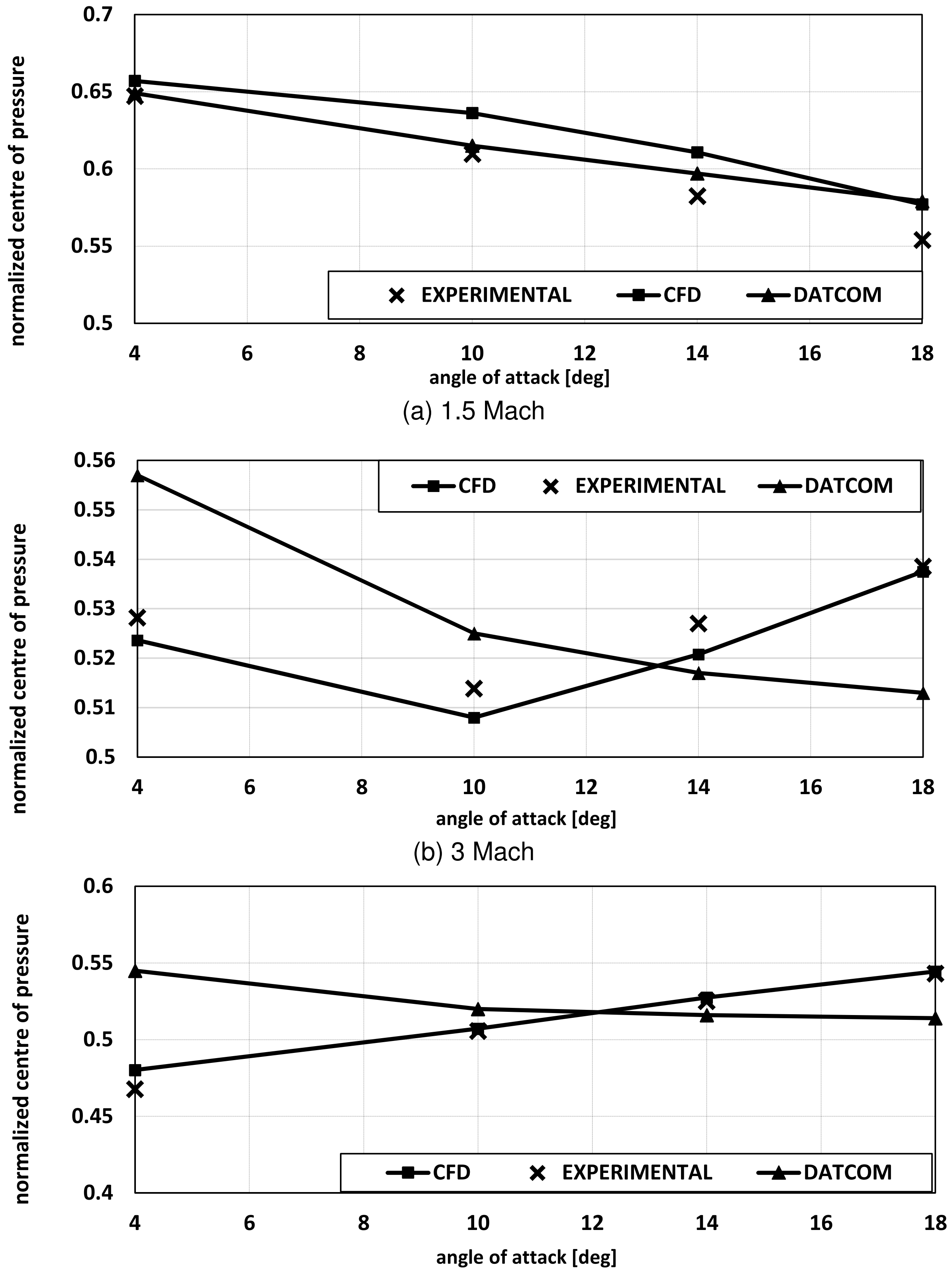

(a) 1.5 Mach

(b) 3 Mach

(c) 4 Mach

Figure 9. Variation of normalized centre of pressure with incidence at different free-stream Mach values.

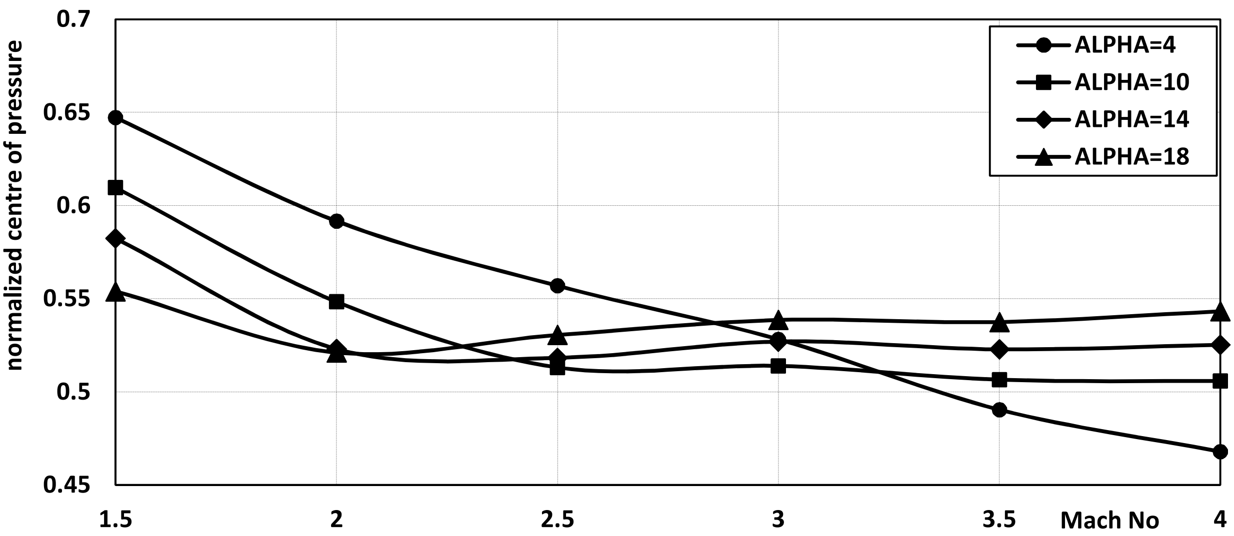

(a) Experimental

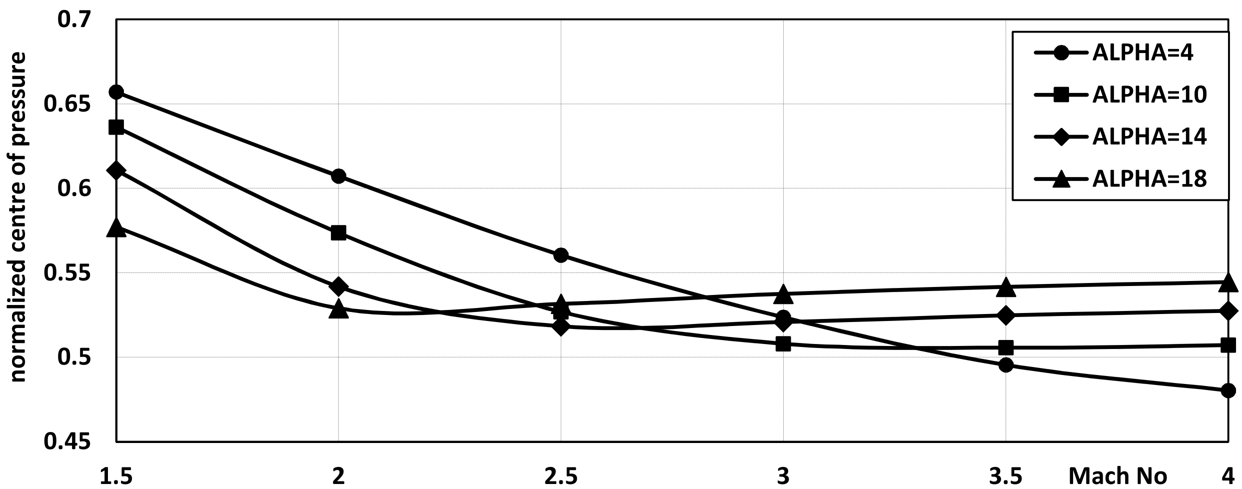

(b) Computational

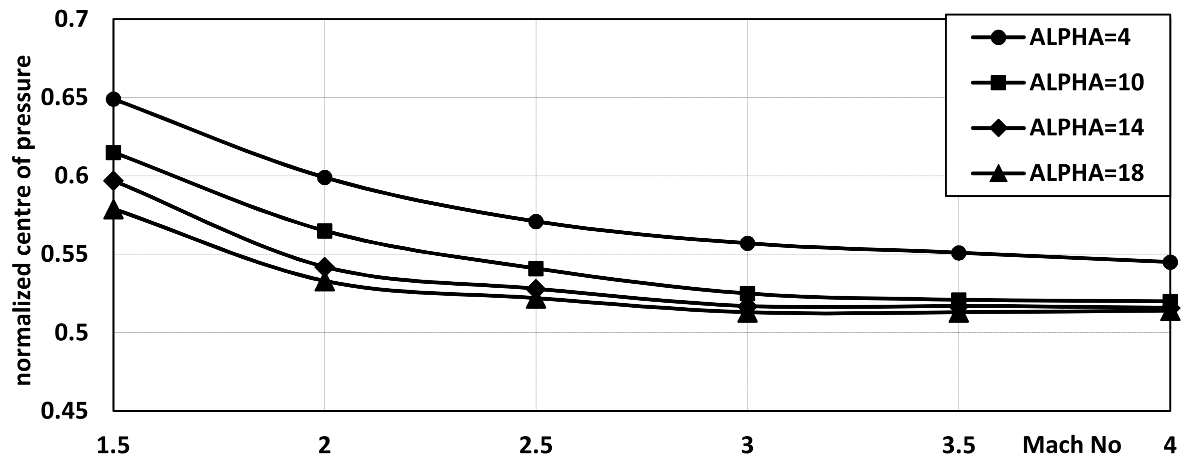

(c) DATCOM

Figure 10. Variation of normalized centre of pressure with incidence at different free stream Mach values.